Chemical Physics Letters 465 (2008) 207–211

Contents lists available at ScienceDirect

Chemical Physics Letters

journal homepage: www.elsevier.com/locate/cplett

Infrared absorption cross-sections for peroxyacyl nitrates (nPANs)

E. Monedero [a], M.S. Salgado [a,*], F. Villanueva [a], P. Martín [a], I. Barnes [b], B. Cabañas [a]

[a] *Departamento de Química Física, Facultad de Ciencias Químicas, Universidad de Castilla La Mancha, Avda Camilo José Cela 10, 13071 Ciudad Real, Spain*
[b] *Physikalische Chemie/FB C, 9, Bergische Universität, Gaußstraße 20, D-42097 Wuppertal, Germany*

ARTICLE INFO

Article history:
Received 25 March 2008
In final form 8 October 2008
Available online 11 October 2008

ABSTRACT

Absorption spectra of peroxyacyl nitrates (nPANs) at room temperature (298 ± 3 K) have been measured in the mid-infrared range (700–2050 cm^{-1}) using an environmental chamber/FTIR absorption system. nPANs are generated in situ as main products in the NO_3 radical reactions with aldehydes. Both peak absorption cross-sections and integrated band intensities for the principal absorption bands in the peroxypropionyl nitrate (PPN), peroxy-*n*-butyryl nitrate (PnBN), peroxy-*n*-valeryl nitrate (PnVN), peroxyacryloyl nitrate (APAN) and peroxycrotonyl nitrate (CPAN) spectra have been derived from quantitative laboratory measurements. Results are compared with literature data when available and in those cases, a good agreement is observed.

1. Introduction

Peroxyacyl nitrates [$RC(O)OONO_2$] play an important role in urban and regional air quality and in tropospheric chemistry. They are usually referred to as nPANs and they have no known direct emission sources and are formed in situ by photochemical reactions involving volatile organic compounds (VOCs), such as aldehydes, and oxides of nitrogen. Thus, aldehydes are eliminated in the atmosphere mainly by photolysis or by the reaction with OH and NO_3 radicals. Both atmospheric oxidants (OH at day-time and NO_3 radicals at night-time) are expected to react preferentially with aliphatic aldehydes through the abstraction of the aldehydic H-atom. These processes will give acyl radicals, RC(O), which combine with O_2 to give acylperoxy radicals $RC(O)O_2$. These radicals rapidly react with NO to give NO_2 which is then photolyzed leading to ozone formation or react with NO_2 to form a stable peroxyacyl nitrate ($RC(O)O_2NO_2$) [1].

The reaction with OH is very slow and constitutes a negligible loss of PAN throughout the troposphere [2]. The rate constant for thermal dissociation, however, has very strong temperature dependence that control atmospheric lifetimes of PANs in the lower troposphere. At NO/NO_2 ratios typical for the troposphere, the lifetime of PAN varies from about 40 min at temperatures of 300 K to several months at temperatures characteristic of the upper troposphere. Thus, PANs are quite stable in the mid-upper troposphere and they can be transported over long distances from polluted continental regions into the remote troposphere such over the Pacific Ocean [3].

Therefore, nPANs species are important in the atmosphere for several reasons. They act as reservoirs of NO_x and are closely related to the photochemical ozone formation and on the oxidising potential of the atmosphere [1,4]. Moreover, the long thermal lifetime of nPANs in the cold upper troposphere allow them to transport NO_2 over wide areas, taking NO_2 from polluted regions and releasing it in remote locations where active nitrogen chemistry can influence the production of surface ozone [5]. Peroxyacyl nitrates have also received regular attention as eye irritants, mutagens, possible agents of skin cancer and phytotoxins [6–11]. But despite its importance, nPANs are not included in urban air quality monitoring networks and long-term trends can only be examined from data obtained in studies carried out in recent years [12,13].

Measurements of nPAN and its homologues have most often been accomplished by gas chromatography with electron capture detection (GC-ECD) [12–18]. However, the infrared technique of measuring trace gases in the air has been evolving with rapid progress during last years [19]. IR spectroscopy could provide an alternative to remotely detect trace organic species such as nPANs by virtue of their characteristic infrared signature and to determine global concentrations. It could be an alternative measurement method to the electron capture gas chromatography avoiding the problem of the thermal decomposition of nPANs [20].

In this Letter, using an environmental chamber/FTIR absorption system, we identify the night-time processes of generation of some nPANs [$RC(O)OONO_2$]: peroxypropionyl nitrate (PPN, $R = CH_3CH_2–$), peroxy-*n*-butyryl nitrate (PnBN, $R = CH_3(CH_2)_2–$), peroxy-*n*-valeryl nitrate (PnVN, $R = CH_3(CH_2)_3–$), peroxyacryloyl nitrate (APAN, $R = CH_2{=}CH–$) and peroxycrotonyl nitrate (CPAN, $R = CH_3–CH_2{=}CH–$) in the atmosphere due to the reaction of NO_3 radical with aldehydes (propionaldehyde, *n*-butyraldehyde, *n*-valeraldehyde, acrolein (prop-2-en-1-al) and crotonaldehyde (but-2-en-1-al)) respectively. Using the infrared spectra obtained for the considered compounds, peak absorption cross-sections and integrated band intensities of the peroxyacyl nitrates formed have been

---

* Corresponding author. Fax: +34 926295318.
E-mail address: Sagrario.salgado@uclm.es (M.S. Salgado).

0009-2614/$ - see front matter © 2008 Elsevier B.V. All rights reserved.
doi:10.1016/j.cplett.2008.10.020

determined. These data will provide a useful spectral reference dataset for investigations of the potential for retrieval of concentration information for these compounds from IR spectra of the Earth's atmosphere.

2. Experimental method

All of the experiments were carried out in a 405 L Pyrex cylindrical glass reactor (1.5 m length and 60 cm inner diameter) with Teflon coated metal end flanges. This reactor has previously been described in detail [21]. In brief, a white mirror system (base path length 1.4 m) mounted inside the reactor is coupled, by an external mirror system, to a Fourier transform-spectrometer (Nicolet Magna 550) and this arrangement enables the *in situ* monitoring of both reactants and products by long-path infrared absorption using a total pathlength of 50.4 m and a resolution of 1 cm^{-1}. The spectrometer was directly controlled by OMNIC software provided by Nicolet and running on a personal computer, which was also used to store raw data.

Nitrate radicals were generated by thermal decomposition of N_2O_5. The N_2O_5 was synthesized in a separate setup by the reaction of excess O_3 with NO_2 and trapped and stored at 195 K.

First, to obtain the wall losses, the organic compound was introduced alone into the reaction chamber under reduced pressure and the wall loss rate (k_3) for the compound was derived from the slope of plots of $\ln([C_0]/[C_t])$ against time, where C_0 is the initial concentration of the compound at $t = 0$ and C_t its concentration at time t. For the studied compounds, wall deposition losses were estimated to be negligible (10^{-5}–10^{-6}) s^{-1}, although this was corrected in the experiments. After this determination, N_2O_5 was flushed into the chamber through a Teflon line by evaporating solid N_2O_5. In total, the measurement time period for one experiment was about 30 min, with 128 scans recorded per spectrum over a period of 2 min and 15 such spectra collected. Once the N_2O_5 has been consumed, possible wall deposition of the products formed was studied as described above and once again the losses were negligible.

The experiments were conducted at total pressure of 760 ± 10 Torr (synthetic air) and at a temperature of 298 ± 3. The initial aldehydes concentration range was $(0.3–8.9) \times 10^{14}$ molecule cm^{-3} and the initial N_2O_5 concentration range was $(1.4–6.3.1) \times 10^{13}$ molecule cm^{-3}. Initial NO_2 concentration range was $(0.5–7.6) \times 10^{13}$ molecule cm^{-3}.

The analysis of the complex spectra and the quantification of reactant and products were carried out by comparison with Quantitative reference spectra of the organic compounds, N_2O_5, NO, NO_2, HNO_3, HCHO and CO, which were taken from a calibrated infrared spectra data bank archived by the laboratory. The known concentration of the reference spectra and the subtraction factors allowed the concentration of each identified compound to be determined.

In the case of peroxyacyl nitrates, their spectra were obtained from the final product spectrum of the reaction after the absorption bands of the identified products and reactants were subtracted. nPANs were identified by comparison with reference spectra previously published when available [22–25]. This residual spectrum (Fig. 1 in the case of PPN compared with reference one) shows several intense absorptions at around 796, 1037, 1300, 1741 and 1834 cm^{-1}, which are characteristic of the NO_2 scissors, NO_2 symmetric stretch, NO_2 asymmetric stretch, and CO stretching modes, respectively, in peroxyacyl nitrates.

Chemicals used in this study and their sources and purities were as follows: synthetic air 99.99%, NO_2 98% (in volume), NO 99.5%, O_2 99.95%, supplied by Messer-Griesheim. Organics: propionaldehyde 99%, *n*-butyraldehyde 99%, *n*-valeraldehyde 97%, acrolein 99% and crotonaldehyde 99% were supplied by the Aldrich Chemical Co. and purified by successive trap-to-trap distillations.

3. Results and discussion

3.1. Peak absorption cross-sections

The peak cross-sections calculation for PPN, PnBN y PnVN is similar, and we will explain as example the procedure in the case of PPN.

PPN is clearly the sole significant product obtained in the reaction of propionaldehyde with NO_3. Assuming yields of 100% for this product and neglecting all potential losses, it is reasonable to determine PPN concentrations using propionaldehyde consumption during the experiment. The intensities of the absorption features observed in the product spectra at 796, 1050, 1304, 1738 and 1835 cm^{-1} grew proportionally (i.e. their relative intensities remained constant) and they are all due to PPN. Therefore, the peak absorption cross-section at each wavelength was obtained as the slope of plots of the infrared absorbance as a function of the prod-

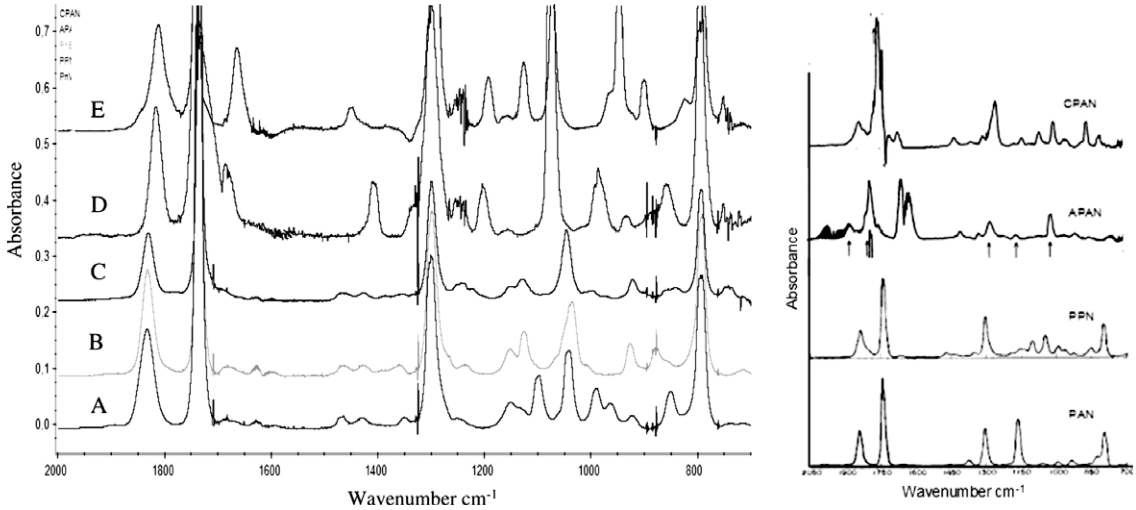

Fig. 1. *Left trace*: infrared residual absorption spectra observed of the reaction of NO_3 with propionaldehyde (A, assigned to PPN), *n*-butyraldehyde (B, assigned to PnBN), *n*-valeraldehyde (C, assigned to PnVN), acrolein (D, assigned to APAN) and crotonaldehyde (E, assigned to CPAN), after subtraction process. *Right trace*: literature spectra of PAN, PPN, APAN and CPAN for comparison [24,26]. Some small contaminants can be seen but it was impossible to remove completely. That is one of the reasons that we assumed 15% error in subtraction process. Complete spectra data base is available in Ref. [31].

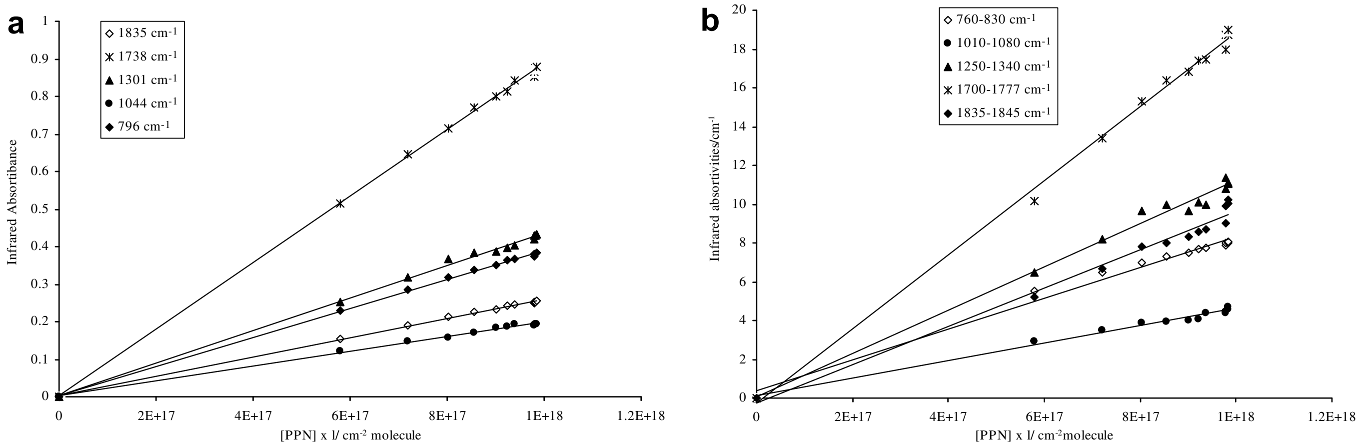

Fig. 2. (a) Infrared absorbance taken at the quoted band centre as a function of PPN concentration × pathlength. (b) Integrated band area vs [PPN] × pathlength, for each of the wavenumber interval due to PPN.

Table 1

Wavenumbers (cm^{-1})	PPN	PnBN	PnVN	APAN	CPAN
793				(10.8 ± 3)[a]	(13.1 ± 0.2)[a]
796	(9.04 ± 0.09)[a]	(5,40 ± 0.09)[a]	(7.31 ± 0.14)[a]		
950					(6.95 ± 0.3)[a]6.5[b]
1037		(2.59 ± 0.05)[a]			
1044	(2.76 ± 0.09)[a]				
1050			(4,.4 ± 0.03)[a]		
1070				(15.6 ± 0.7)[a]18[b]	
1193					(2.14 ± 0.1)[a]1.8[b]
1205				(2.88 ± 0.2)[a]3.4[b]	
1300		(5.76 ± 0.12)[a]		(11.2 ± 0.3)[a]13[b]	(12.5 ± 0.3)[a]11[b]
1301	(10.1 ± 0.2)[a]				
1304			(7.84 ± 0.2)[a]		
1738			(1.98 ± 0.30)[a]		
1738	(20.6 ± 0.2)[a]				
1740					(28,5 ± 0.4)[a]32[b]
1741		(14.5 ± 0.2)[a]			
1748				(24.2 ± 1)[a]28[b]	
1810					(6.84 ± 0.1)[a]6[b]
1818				(7.78 ± 0.5)[a]8.0[b]	
1832			(4.66 ± 0.04)[a]		
1834		(3.63 ± 0.06)[a]			
1835	(5.97 ± 0.07)[a]				

[a] Peak absorpBUGH Wuppertal, Wuppertaltion cross-section (in units 10^{-19} $molecule^{-1}$ cm^2), for PPN, PnBN, PnVN, APAN and CPAN determined in this work.

[b] Values previously determined for APAN and CPAN [26].

uct of PPN concentration with the optical pathlength according to Lambert–Beer's law. Fig. 2a shows these plots for each of the wavenumber due to PPN. Similar plots could be obtained for the calculations of the peak absorption cross-sections of PnBN and PnVN. Values determined are shown in Table 1. The errors quoted represent the two standard deviation errors (2σ) calculated from Beer's law fits at the bands centres. Because wall loss deposition rates were already considering in the calculations, the main systematic uncertainty arose from uncertainties in the FTIR subtraction procedure and is considered about 15%. No other values for peak absorption cross-sections for these compounds have previously been published.

For APAN and CPAN peak cross-sections evaluation there are several differences. Thus, in the NO_3 radical-initiated oxidation of acrolein, formaldehyde, CO and acryloylperoxy nitrate (APAN) were the main reaction products detected [25]. In order to determine the concentration of APAN we estimated that all acrolein consumed was used to form HCHO, CO and APAN (because other products are not observed in a significant way). The concentration of CO and HCHO could be calculated using calibrated spectra for these compounds and, therefore, from the difference with acrolein consumed we can ascertain the concentration of APAN. The same procedure was followed in the case of the reactions of crotonaldehyde with NO_3 where crotonylperoxy nitrate (CPAN) and CO were detected as products [25]. APAN and CPAN were identified by comparison with a reference spectrum [26]. Values of peak absorption

Table 2

Peroxypropionyl nitrate integrated band intensities (IBI, cm^2 $molecule^{-1}$ cm^{-1}) compared with bibliographic references.

Band (cm^{-1})	Integrated band strength (cm^{-1})	Gaffney et al. [24]	Le Crane et al. [30]	This work
796	760–830	1.97×10^{-17}	2.00×10^{-17}	$(1.83 \pm 0.7) \times 10^{-17}$
1044	1010–1080	1.23×10^{-17}	1.17×10^{-17}	$(1.04 \pm 0.5) \times 10^{-17}$
1301	1250–1340	2.86×10^{-17}	2.88×10^{-17}	$(2.56 \pm 0.1) \times 10^{-17}$
1738	1700–1777	5.03×10^{-17}	5.16×10^{-17}	$(4.40 \pm 0.9) \times 10^{-17}$
1835	1777–1880	2.45×10^{-17}	2.6×10^{-17}	$(2.29 \pm 0.5) \times 10^{-17}$

Table 3
Integrated band intensities (IBI) calculated in this work for PnBN and PnVN and spectral ranges used for calculations.

PnBN			PnVN		
Band (cm^{-1})	Integrated band strength (cm^{-1})	IBI/cm^2 ($molecule^{-1}$ cm^{-1})	Band (cm^{-1})	Integrated band strength (cm^{-1})	IBI/cm^2 ($molecule^{-1}$ cm^{-1})
796	763–849	$(2.56 \pm 0.05) \times 10^{-17}$	796	764–825	$(1.20 \pm 0.10) \times 10^{-17}$
1037	980–1185	$(3.52 \pm 0.20) \times 10^{-17}$	1050	1010–1187	$(1.45 \pm 0.15) \times 10^{-17}$
1300	1223–1340	$(3.62 \pm 0.2) \times 10^{-17}$	1304	1270–1350	$(1.82 \pm 0.14) \times 10^{-17}$
1741	1777–1691	$(5.80 \pm 0.2) \times 10^{-17}$	1738	1705–1773	$(3.16 \pm 0.11) \times 10^{-17}$
1834	1777–1880	$(2.33 \pm 0.05) \times 10^{-17}$	1832	1773–1873	$(1.21 \pm 0.17) \times 10^{-17}$

Table 4
Integrated band intensities (IBI) calculated in this work for APAN and CPAN and spectral ranges used for calculations.

APAN			CPAN		
Band (cm^{-1})	Integrated band strength (cm^{-1})	IBI/cm^2 ($molecule^{-1}$ cm^{-1})	Band (cm^{-1})	Integrated band strength (cm^{-1})	IBI/cm^2 ($molecule^{-1}$ cm^{-1})
793	769–818	$(2.42 \pm 0.07) \times 10^{-17}$	793	765–812	$(1.91 \pm 0.08) \times 10^{-17}$
1070	1047–1104	$(2.84 \pm 0.07) \times 10^{-17}$	950	930–986	$(8.12 \pm 0.3) \times 10^{-19}$
1205	1180–1220	$(4.49 \pm 0.02) \times 10^{-18}$	1193	1175–1215	$(4.90 \pm 0.2) \times 10^{-18}$
1300	1265–1332	$(2.53 \pm 0.1) \times 10^{-17}$	1300	1270–1328	$(2.95 \pm 0.1) \times 10^{-17}$
1748	1734–1763	$(5.20 \pm 0.4) \times 10^{-18}$	1740	1730–1760	$(2.68 \pm 0.1) \times 10^{-17}$
1818	1792–1843	$(1.40 \pm 0.05) \times 10^{-17}$	1810	1780–1847	$(1.71 \pm 0.07) \times 10^{-17}$

cross-section determined here for APAN and CPAN are also shown in Table 1. Values obtained are in good agreement with previously determined for these compounds (also presented in the table) by Orlando and Tyndall [26] with deviation always lower than 15%. Additionally, we used the absorption cross-sections previously calculated by Orlando and Tyndall [26] for calculation of APAN and CPAN concentrations in our experiments, and similar results have been obtained, confirming the reliability of the calculation method of concentrations.

3.2. Integrated band intensities (IBI) calculation

Integrated band areas at room temperature of the five principal absorption bands obtained for peroxyacyl nitrates were determined by integrating over the wavenumber covered by the absorption band of interest. Once the integrated band area was determined, the plot of these values versus ([peroxyacyl nitrate] × pathlength) allowed us to obtain the integrated band intensities (IBI) as the slopes of the least squares linear regression fits. Fig. 2b shows this plot in the case of PPN. Similar plots could be obtained for the calculations of the integrated band intensities of PnBN, PnVN, APAN and CPAN that have similar absorption bands in the IR region.

There are several studies concerning to IBI calculations for peroxyacetyl nitrate PAN and for peroxypropionyl nitrate PPN [24,26–30]. Reference IBI values for PPN are compared with the ones obtained in our experimental study in Table 2. As it can be seen in the table, within the stated errors, our data are in good agreement with other calculations (deviation always lower than 15%). Table 3 summarizes obtained results for PnBN and PnVN although, to date, no other calculations of the integrated band intensities of these compounds are available in literature. Reasonability, we expect that the values of Integrated Band Intensities calculated for PnBN and PnVN are well determined.

Integrated band intensities of APAN and CPAN are listed in Table 4. This is also the first time that these values have been achieved. Due to the good agreement (deviation always lower than 15%) of peak absorption cross-sections for these compounds with previously determined by Orlando and Tyndall [26], we confirm again the reliability of the IBI values determined.

The infrared absorption cross-sections determined here will increase the available database required for calculation of atmospheric nPANs concentrations, indicating that IR spectroscopy could provide an alternative technique to remotely detect trace organic species by virtue of their characteristic infrared signature and then to determine global concentrations. For nPANs evaluation, it is important to consider, when quantitative determinations were made, the overlapping bands observed in the spectra reported here.

Acknowledgments

Esperanza Monedero and Florentina Villanueva thanks to the 'Ministerio de Educación y Cultura' and Junta de Comunidades de Castilla La Mancha respectively, for personal grants. This work was supported by the project BQU-2001-1574 granted by the C.I.C.Y.T ('Comisión Interministerial de Ciencia y Tecnología'). The authors also thank the cooperation of the Wuppertal University, especially the Physikalische Chemie for the possibility of developing these experiments.

References

[1] R. Atkinson, Atmos. Environ. 34 (2000) 2063.
[2] R.K. Talukdar, S.C. Herndon, J.B. Burkholder, J.M. Roberts, A.R. Ravishankara, J. Chem. Soc. Faraday Trans. 93 (1997) 2787.
[3] F.M. Flocke, A.J. Weinheimer, A.L. Swanson, J.M. Roberts, R. Schmitt, S. Shert, J. Atmos. Chem. 52 (2005) 19.
[4] J.M. Roberts, in: H.B. Singh (Ed.), Composition, Chemistry and Climate of the Atmosphere, Van Nostrand Reinhold, New York, 1995, p. 176.
[5] K.J. Olszyna, E.M. Bailey, R. Simonaitis, J.F. Meagher, J. Geophys. Res.-A. 99 (1994) 14557.
[6] E.R. Stephens, Adv. Environ. Sci. Technol. 1 (1969) 119.
[7] O.C. Taylor, J. Air Pollut. Contr. Assoc. 19 (1969) 347.
[8] M.J. Peak, W.L. Belser, Atmos. Environ. 3 (1969) 385.
[9] T.E. Kleindienst et al., Environ. Mol. Mutagen. 16 (1990) 70.
[10] O.C. Taylor, D.C. MacLean, J.S. Jacobson, A.C. Hill (Eds.), Air Pollution Control Association, Pittsburgh, PA, 1970, p. E1.
[11] J.B. Mudd, in: J.B. Mudd, T.T. Kozlowski (Eds.), Responses of Plants to Air Pollution, Academic Press, New York, 1975, p. 97.

[12] E. Grosjean, D. Grosjean, M. Fraser, G. Cass, Environ. Sci. Technol. 30 (1996) 2704.
[13] E. Grosjean, D. Grosjean, L.F. Woodhouse, Environ. Sci. Technol. 35 (2001) 4007.
[14] H.B. Singh, L.J. Salas, Atmos. Environ. 17 (1983) 1507.
[15] K.P. Müller, J. Rudolph, J. Environ. Anal. Chem. 37 (1989) 253.
[16] W. Schrimpf, K.P. Muller, F.J. Johnen, K. Lienaerts, J. Rudolph, J. Atmos. Chem. 22 (1995) 303.
[17] A. Volz-Thomas, I. Xueref, R. Schmitt, Environ. Sci. Pollut. Res. 9 (2002) 72.
[18] L.K. Whalley et al., J. Environ. Monit. 6 (2004) 234.
[19] G. Allen, The Infrared Remote Sensing of Peroxyacetyl Nitrate in the Upper Troposphere PhD, Department of Physics and Astronomy, University of Leicester, 2005.
[20] F. Kirchner, A. Mayer-Figge, F. Zabel, K.H. Becker, Int. J. Chem. Kinet. 31 (1999) 127.
[21] A. Bierbach, Produktuntersuchungen und Kinetik der OH-initiierten Gasphasenoxidation aromatischer Kohlenwasserstoffe sowie ausgewähter carbonyllischer Folgenprodukte, Ph.D. dissertation, BUGH Wuppertal, Wuppertal, 1994.
[22] J.F. Doussin, B. Picquet-Varrault, R. Durand-Jolibois, H. Loirat, P. Carlier, J. Photochem. Photobiol. A 157 (2003) 283.
[23] J. Bossmeyer, T. Brauers, C. Richter, F. Rohrer, R. Wegener, A. Wahner, Geophys. Res. Lett. 33 (2006) 18810.
[24] J.S. Gaffney, R. Fajer, G.I. Senum, Atmos. Environ. 18 (1984) 215.
[25] M.S. Salgado, E. Monedero, F. Villanueva, P. Martín, A. Tapia, B. Cabañas, Environ. Sci. Technol. 42 (2008) 2394.
[26] J.J. Orlando, G.S. Tyndall, J. Phys. Chem. A 106 (2002) 12252.
[27] G. Allen, J.J. Remedios, D.A. Newnham, K.M. Smith, P.S. Monks, Atmos. Chem. Phys. 5 (2005) 47.
[28] S.A. Nizkorodov, J.D. Crounse, J.L. Fry, C.M. Roehl, P.O. Wennberg, Atmos. Chem. Phys. 5 (2005) 385.
[29] G. Allen, J.J. Remedios, K.M. Smith, Atmos. Chem. Phys. 5 (2005) 3153.
[30] J.P. Le Crâne, E. Villenave, M.D. Hurley, T.J. Wallington, J.C. Ball, J. Phys. Chem. A 109 (2005) 11837.
[31] <http://www.uclm.es/profesorado/mssalgado/Investigacion.htm>.